Thermal diffusion in a binary liquid due to rectified molecular fluctuations

Simon Villain-Guillot, Alois Würger

Thermal diffusion in a binary liquid due to rectified molecular fluctuations

Simon Villain-Guillot and Alois Würger
Laboratoire Ondes et Matière d'Aquitaine, Université Bordeaux 1 & CNRS,
351 cours de la Libération, 33405 Talence, France

The Soret motion in binary liquids is shown to arise to a large extent from rectified velocity fluctuations. From a hard-bead model with elastic collisions in a non-uniform temperature, we derive a net force on each molecule, which is proportional to the temperature gradient and depends on the ratio of the molecular masses and moments of inertia. Our findings agree with previous numerical simulations and provide an explanation for the thermal diffusion isotope effect observed for several liquids.

Non-equilibrium fluctuations may rectify the motion of a Brownian particle and give rise to directed diffusion [1, 2]. Noise-driven transport has been studied extensively in terms of ratchet models, where the broken symmetry is realized by a random force with zero mean and asymmetric spectrum, a saw-tooth like potential with a periodic time-dependent temperature profile, or non-uniform chemical reactions. Applications range from molecular motors to electron transport in quantum devices [2].

The thermal diffusion or Soret effect describes motion due to a temperature gradient [3]. From kinetic theory it is known that in a gas mixture the lighter atoms move to the warm, the heavier ones to the cold [4]. It has been realized early that this effect can be used for isotope separation [5]. In contrast to gases, thermally driven motion in molecular liquids is less well understood [6, 7], despite a variety of available approaches [8–11]. Part of the complexity is due to the presence of two basically different driving mechanisms: The first one results from solute-solvent interactions such as electric-double layer and dispersion forces [12–15], and is particularly relevant for charged colloidal suspensions [16–18]. The second one, which we are interested in here, relies on the thermal fluctuations of solute and solvent molecules.

Since velocity fluctuations are inversely proportional to the mass, they are expected to be most relevant for light molecules or atoms. This is confirmed by the isotope effects observed in experiments on molecular liquids [19–22] and by numerical simulations [23–26]. Thus Debuschewitz and Köhler reported that protonated benzene in cyclohexane migrates to higher temperatures, whereas deuterated benzene goes to the cold side [20]. Even more strikingly, the benzene isotopes $^{12}C_6D_6$ and $^{13}C_6H_6$, which have equal mass but different moment of inertia, vary significantly in their thermal diffusion behavior, thus hinting at the role of rotational diffusion.

In the present paper we study how velocity fluctuations and rotational diffusion affect the Soret effect of a binary liquid. Thermal noise acts as a random force f and results in molecular Brownian motion. In thermal equilibrium the mean force is zero. In a non-equilibrium system, however, its average $F = \langle f \rangle$ does not necessarily vanish and may result in a steady-state velocity

$$u = \frac{F}{\xi}, \tag{1}$$

where the Stokes friction coefficient ξ is given by the correlation $\langle f(t)f(0)\rangle$. Our main purpose is to relate this drift term to the non-uniform temperature that appears in the molecular velocity distribution functions. The random force is described by the momentum Δp transferred from colliding neighbor molecules, $f = \sum_i \Delta p \delta(t - t_i)$. Its average value reads

$$F = \left\langle \frac{\Delta p}{\tau} \right\rangle, \tag{2}$$

where τ is the time separating two subsequent collisions. The conservation laws are evaluated explicitly for a hard-bead model with elastic collisions, giving F as a function of the molecular masses and moments of inertia. The model is shown in Fig. 1, which in particular illustrates the importance of translation-rotation coupling for non-spherical molecules.

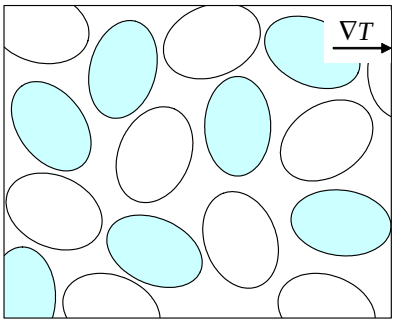

FIG. 1: Schematic view of a binary liquid of non-spherical molecules. The two species have equal volume but different mass and different moment of inertia.

In the absence of an external potential, the weighted average of the forces F_a and F_b exerted on each component vanishes. For molecules of equal size this condition simplifies to

$$\phi_a F_a + \phi_b F_b = 0, \tag{3}$$

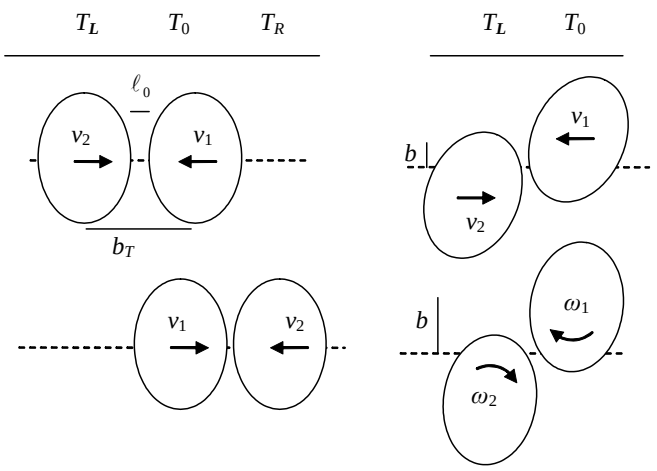

FIG. 2: Schematic view of two-particle elastic collisions. The left panel shows a frontal impact with the second particle coming from the left ($v_2 > v_1$) or from the right ($v_2 < v_1$). Because of the non-uniform temperature, the velocity distribution of each particle is with respect to a particular value, $T_L < T_0 < T_R$. In terms of the constant gradient ∇T, the differences read $\pm b_T \nabla T$. The right panel shows the case of non-zero impact parameter b. The upper example illustrates an initial state with linear velocity and zero angular velocity ($\omega_i = 0$), and the lower one the opposite case with finite ω_i and zero v_i. In both cases linear momentum Δp is transferred during the collision, according to Eq. (11). Only collisions from the left side are shown.

where the volume fractions satisfy $\phi_a + \phi_b = 1$. The momentum transfer Δp depends on the linear and angular velocities of both molecules. Elastic collisions of two rigid particles satisfy the conservation laws

$$\begin{aligned} E_1' + E_2' &= E_1 + E_2, \\ p_1' + p_2' &= p_1 + p_2, \\ \sigma_1' + \sigma_2' &= \sigma_1 + \sigma_2, \end{aligned} \tag{4}$$

where $p_i = m_i v_i$ denotes the linear momentum, σ_i the angular momentum, and $E_i = p_i^2/2m_i + \sigma_i^2/2I_i$ the kinetic energy with the moment of inertia I_i. The primed quantities describe the state after the collision. In three dimensions there are seven independent equations for twelve unknown variables; an unambiguous final state is determined by five additional conditions for the collision.

Here we study a one-dimensional model where p and σ are taken as scalars. In a first approach we neglect the angular momentum and consider frontal collisions only, as illustrated in the left panel of Fig. 2. From the conservation laws for E and p, one readily obtains the momentum transfer $\Delta p = p_1' - p_1$ in terms of the initial state,

$$\Delta p = 2\mu_{12}(v_2 - v_1), \tag{5}$$

with the reduced mass $1/\mu_{12} = 1/m_1 + 1/m_2$.

A net force arises from the fact that the thermal average in (2) has to be done with a particular temperature for each particle. The position of molecule 1 defines a reference temperature T_0, whereas that of particle 2 may be lower or higher, depending on its relative position, as illustrated in the left panel of Fig. 2. As an important quantity, the collision rate $1/\tau$ is a function of temperature and velocity. In order to keep the algebra as simple as possible, we adopt from the beginning the form

$$1/\tau = |v_2 - v_1|/\ell, \tag{6}$$

which is proportional to the relative velocity. The momentum transfer is positive for collisions from the left, that is for $v_2 > v_1$; inserting Δp and the rate in (2) one finds

$$\left\langle \frac{\Delta p}{\tau} \right\rangle_L = 2\mu_{12} \int_{-\infty}^{\infty} dv_1 \int_{v_1}^{\infty} dv_2 \varphi_1 \varphi_2 \frac{(v_2 - v_1)^2}{\ell_L},$$

with the Maxwell velocity distribution function $\varphi(v) = (2\pi\langle v^2\rangle)^{-\frac{1}{2}} e^{-\frac{1}{2}v^2/\langle v^2\rangle}$. A similar expression of opposite sign arises from neighbor molecules coming from the right, where $v_2 < v_1$. Because of the spatial variation of temperature and of the parameter ℓ, these contributions do not completely cancel each other. Their difference gives the net force on particle 1,

$$F_1 = \mu_{12} \left(\frac{\langle v_1^2\rangle_0 + \langle v_2^2\rangle_L}{\ell_L} - \frac{\langle v_1^2\rangle_0 + \langle v_2^2\rangle_R}{\ell_R} \right), \tag{7}$$

where $0, L, R$ indicate the molecular position.

Now we determine the temperature dependence of the mean spacing ℓ. We insert (7) with the mean velocity square $\langle v_i^2\rangle_X = k_B T_X/m_i$ in the constraint (3). Performing for both molecules 1 and 2 the average with respect to the species a and b, we obtain the condition

$$(T_0 + T_L)/\ell_L = (T_0 + T_R)/\ell_R, \tag{8}$$

which means that ℓ is determined by the mean temperature of the colliding molecules. This relation could be obtained equally well by requiring that the net force vanishes in a pure system, in other words, by putting $F = 0$ for an a-molecule in an a-environment.

The physical origin of the thermal force is best discussed in terms of the velocity fluctuations appearing in (7). Its positive and negative contributions arise from collisions with molecules at the left or at the right, with $T_L < T_R$. If particle 1 is much lighter than 2 ($m_1 \ll m_2$), its mean square $\langle v_1^2\rangle_0 = k_B T_0/m_1$ dominates the numerators and, because of $\ell_L < \ell_R$, leads to a positive force to the hot side. In the opposite case $m_1 \gg m_2$, the numerators are proportional to T_L and T_R; since $\ell(T)$ varies more weakly with T, the second term in (7) exceeds the first one, and the force takes a minus sign. Thus the temperature gradient acts like a rectifier on the molecular velocity fluctuations, which drives the heavier component to lower T, and the lighter one to the hot side.

Eq. (8) can be rewritten as $\ell = \ell_0(T + T_0)/2T_0$, with constant ℓ_0. Replugging this expression in the force on

an a-molecule, averaging the collision partner 2 with respect to composition, and expanding to linear order in the temperature variation, we find

$$F_a = \phi_b \frac{b_T}{\ell_0} \frac{m_b - m_a}{m_b + m_a} k_{\rm B} \nabla T. \qquad (9)$$

Here we have used $T_{R/L} = T_0 \pm b_T \nabla T$ as defined in Fig. 2. The force on a molecule of the second species is obtained by exchanging the labels a and b; one readily verifies the condition (3). It is noteworthy that F_a vanishes in a pure a-system ($\phi_b = 0$) and is maximum in a b-environment ($\phi_b = 1$). Our expresson for F_a compares favorably with early work for heavy Brownian particles, where $F = -k_{\rm B}\nabla T$ [28]. This corresponds to our Eq. (9) for $m_a \gg m_b$ and $b_T = \ell_0$. The latter parameters are related to the molecular structure, which is hardly addressed in [28].

Now we take the angular momentum into account. Besides the three conservation laws (4), there is one condition relating the changes of momentum and angular momentum $\Delta\sigma = \sigma_1' - \sigma_1$. In the one-dimensional model it takes the simple form

$$\Delta\sigma = b\Delta p, \qquad (10)$$

where b is an impact parameter as illustrated in the right panel of Fig. 2. The four equations (4) and (10) determine the final state p_i', σ_i' in terms of the incoming quantities p_i, σ_i, with the angular momentum $\sigma_i = I_i\omega_i$. In view of (2) we are mainly interested in the momentum transfer, and thus give its explicit expression

$$\Delta p = \frac{2}{1/\mu_{12} + b^2/\mathcal{I}_{12}} \left[v_2 - v_1 + b(\omega_2 - \omega_1)\right], \qquad (11)$$

with the reduced moment $\mathcal{I}_{12}^{-1} = I_1^{-1} + I_2^{-1}$. For non-zero b both linear and angular velocities result in momentum transfer, as illustrated in the right panel of Fig. 2. In analogy to (6), the collision rate reads $1/\tau = |v_2 - v_1 + b(\omega_2 - \omega_1)|/\ell$,

We consider separately collisions with non-zero velocities v_i and angular velocities ω_i. The first case is identical to the analysis between Eqs. (5) and (9), with the reduced mass replaced by the denominator in (11). Proceeding in the same way for the second case, where the center of mass of both moelcules is initially at rest ($v_i = 0$), we merely have to replace the linear velocities v_i with $b\omega_i$. Inserting the mean square $\langle\omega_i^2\rangle = k_{\rm B}T/I_i$ leads to a force similar to that of the first case, but with the moments of inertia instead of the masses.

Adding the contributions calculated independently for the cases $\omega_i = 0$ and $v_i = 0$, we have

$$F_a = -\phi_b \frac{b_T}{\ell_0} \Psi k_{\rm B} \nabla T, \qquad (12)$$

with the shorthand notation for the relative differences of mass and inertia,

$$\Psi = \frac{m_a^{-1} - m_b^{-1} + b^2(I_a^{-1} - I_b^{-1})}{m_a^{-1} + m_b^{-1} + b^2(I_a^{-1} + I_b^{-1})}. \qquad (13)$$

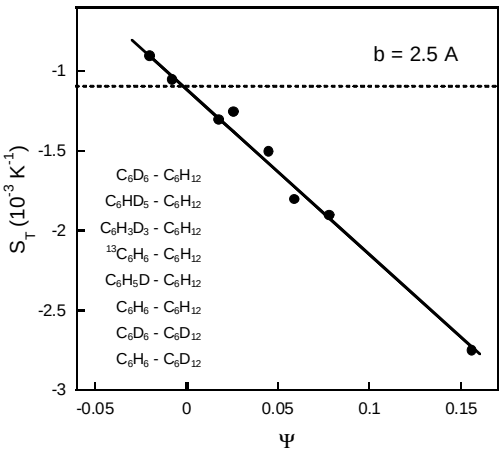

FIG. 3: Isotope effect on the Soret coefficient S_T of benzene-cyclohexane mixtures. Black points are Debuschewitz and Köhler's experimental data at equal mole fractions [20]. The list of isotopes corresponds to the eight data points from the left to the right. The solid line is calcatuled from Eq. (14) with the ratio $b_T/\ell_0 = 3.4$ and the impact parameter $b = 2.5$ Å; the values of m_i and I_i are taken from [20]. The vertical off-set $S_T^0 = -1.1 \times 10^{-3}{\rm K}^{-1}$ is indicated by the dashed line. With benzene as a-molecules, the first two data points correspond to $\Psi > 0$, and the remaining ones to negative Ψ.

For $b = 0$ we recover (9). In principle, this expression should be averaged over the parameters b, b_T, ℓ_0. Moreover, in a general initial state both linear and angular velocities take non-zero values and should be considered simultaneously in (2). These modifications would encumber the algebra without significantly modifying the net force.

Now we discuss the steady state resulting from the the drift velocity (1) and diffusion with the Einstein coefficient $D = k_{\rm B}T/\xi$. The current of the component a reads $J_a = -D\nabla\phi_a + \phi_a u_a$ and is opposite to that of b-molecules. The steady-state condition $J_a = 0$ may be rewritten as [3]

$$\nabla\phi_a + \phi_a\phi_b S_T \nabla T = 0,$$

where the Soret coefficient S_T describes the stationary non-uniform composition of the binary system. With this sign convention, a-molecules accumulate at lower temperature for $S_T > 0$ and at higher T for $S_T < 0$. From (1) and (12) one readily derives

$$S_T = S_T^0 + \frac{b_T}{\ell_0} \frac{\Psi}{T_0}, \qquad (14)$$

where we have added a term S_T^0 that accounts for molecular dispersion forces. Eqs. (12) and (14) consitute the main result of the present paper.

In Fig. 3 we plot data of Debuschewitz and Köhler for mixtures of benzene and cyclohexanė [20]. Studying various isotopes that range from deuterated benzene

and protonated cyclohexane (C_6D_6-C_6H_{12}) to the opposite case C_6H_6-C_6D_{12}, these authors observed a strong mass effect of the Soret coefficient S_T. Since the isotopes have very similar chemical properties and, in particular, the same van der Waals interaction potential, these data show unambiguously that thermal diffusion varies with both molecular mass and moment of inertia. The dependence on the latter quantity is best displayed by comparing deuterated benzene C_6D_6 and the protonated heavy-carbon isotope $^{13}C_6H_6$: These molecules have equal mass but different moment of inertia; their S_T values differ by about 50 %.

The solid line in Fig. 3 is calculated from Eq. (14). With $I_i/m_i \approx 2.5$ Å^2 for benzene and cyclohexane [20], the value for the impact parameter $b = 2.5$ Å implies that the angular velocity fluctuations $k_B T b^2/I_i$ are several times larger than the linear ones $k_B T/m_i$. Thus the quantity Ψ is determined by the moments of inertia rather than by the masses. In physical terms this means that the Soret effect is mainly due to rotational diffusion with the mean square angular velocity $\langle \omega_i^2 \rangle = k_B T/I_i$.

The vertical offset S_T^0 describes thermally driven motion due to dispersion forces and thus is insensitive to a change of the molecular mass; its numerical value is taken from [20]. Thus the Soret coefficient (14) consists of two terms, one of which depends on the composition and the other one on the molecular mass and inertia only [20, 21]. This is confirmed by several experiments that show that the mass and composition dependence of S_T separates in additive contributions [20, 21]. For components of comparable size, a linear variation of S_T^0 with the volume fraction ϕ has been observed in accordance with simulations [27] and a simple mean-field model [15].

The Soret coefficient (14) agrees with numerical simulations of Lennard-Jones and hard-bead systems. Several authors reported dependencies on mass and moment of inertia similar to (13) [23–26]. The ratio of the molecular mean distance b_T and mean spacing ℓ_0 is related to the filling factor; the linear variation of (14) compares favorably with simulation results at different densities [25]. The numerical value of b_T/ℓ_0 used in Fig. 3 agrees with the molecular size $b_T \sim 4$ Å and the spacing between particles $\ell_0 \sim 1$ Å.

The present one-dimensional hard-bead model considerably simplifies the otherwise complex molecular collisions. The rectification of thermal fluctuations, as expressed by the mean-square velocities at different temperatures in Eq. (7), is insensitive to the model details and results in a net force proportional to ∇T with the coefficient Ψ. The agreement of Eq. (14) with the isotope data and with numerical simulations [23–26] confirms that thermal diffusion in binary liquids is to a large extent driven by rectified molecular fluctuations. Though similar effects are expected to occur in macromolecular solutions [30], one should keep in mind that a polymer cannot be treated as a rigid body, thus requiring a refined picture for its collisions with solvent molecules.

[1] R. D. Astumian, Science **276**, 917 (1997)
[2] P. Hänggi, F. Marchesoni, Rev. Mod. Phys. **81**, 387 (2009)
[3] S.R. de Groot, P. Mazur, *Non-equlibrium Thermodynamics*, North Holland Publishing, Amsterdam (1962)
[4] S. Chapman, T. Cowling, *The Mathematical Theory of Non-uniform Gases* (Cambridge University Press, 1970)
[5] W.H. Furry, R.C. Jones, L. Onsager, Phys. Rev. **55**, 1083 (1939)
[6] W. Köhler, S. Wiegand, *Thermal Nonequilibrium Phenomena in Fluid Mixtures*, Lecture Notes in Physics Vol. 584 (Springer 2002)
[7] S. Wiegand, J. Phys. Cond. Matt. **16**, 357 (2004)
[8] E. Dougherty, H. Drickamer, J. Phys. Chem. **59**, 443 (1955)
[9] H. Brenner, Phys. Rev. E **74**, 036306 (2006)
[10] M. Eslamian, M.Z. Saghir, Phys. Rev. E **80**, 0661201 (2009)
[11] K.I. Morozov, Phys. Rev. E **79**, 031204 (2009).
[12] E. Ruckenstein, J. Colloid Interface Sci. **83**, 77 (1981)
[13] K.I. Morozov, J. Exp. Theor. Phys. **88**, 944 (1999)
[14] A. Würger, Phys. Rev. Lett. **101**, 108302 (2008).
[15] A. Würger, Rep. Prog. Phys., **73** 126601 (2010)
[16] R. Piazza, A. Guarino, Phys. Rev. Lett. **88**, 208302 (2002)
[17] S.A. Putnam, D.G. Cahill., Langmuir **21**, 5317 (2005)
[18] S. Duhr, D. Braun, Proc. Natl. Acad. Sci. **103**, 19678 (2006)
[19] W.M. Rutherford, J. Chem. Phys. **81**, 6136 (1984)
[20] C. Debuschewitz, W. Köhler, Phys. Rev. Lett. **87**, 055901 (2001)
[21] G. Wittko, W. Köhler, J. Chem. Phys. **123**, 014506 (2005)
[22] F. Huang et al., Nature **464**, 396 (2010)
[23] F. Müller-Plathe, D. Reith, Comp. Theor. Polym. Sci. **9**, 203 (1999)
[24] G. Galliero et al., Fluid Phase Eq. **208**, 171 (2003)
[25] S. Yeganegi, M. Zolfaghari, Fluid Phase Eq. **243**, 161 (2006)
[26] G. Galliero, S. Volz, J. Chem. Phys **128**, 064505 (2008)
[27] P.-A. Artola, B. Rousseau, Phys. Rev. Lett. **98**, 125901 (2007)
[28] G. Nicolis, J. Chem. Phys. **43**, 1110 (1965)
[29] P. Blanco, P. Polyakov, M. Mounir Bou-Ali, S. Wiegand, J. Phys. Chem. B **112**, 8340 (2008)
[30] A. Würger, Phys. Rev. Lett. **102**, 078302 (2009)